Supplement for: Review of Stress Calculations for Crevasse Depths and Testing with Velocity Prediction Capability

Benjamin Reynolds[1], Sophie Nowicki[1, 2], Kristin Poinar[1, 2]

[1]Department of Geology, University at Buffalo, Buffalo, NY 14260, USA
[2]RENEW Institute, University at Buffalo, Buffalo, NY 14260, USA

Correspondence to: Benjamin Reynolds (br77@buffalo.edu)

S1: Firn density considerations

We did not take firn density into consideration in the surface crevasse depth calculations. Because the surface topography included with BedMachine is corrected for firn density, the amount of ice in terms of integrated density that the crevasse extends through will be the same. (This is true because we used the Nye crevasse theory. The geometry driven changes in stress intensity factor included in LEFM would mean that the integrated density of ice above the crevasse tip would change.) This will give a lower fraction of penetration for the surface crevasse. However, the lower rigidity of firn would tend to reduce this effect by making the extra penetrated length a lower fraction of the total rigidity of the ice column. Lai et al. (2020) show this in their supplement. More importantly, however, basal crevasses make up most of the total crevasse penetration (see Table 4 in the main text).

S2: Sample Temperature Profile

Fig. S1 shows the temperature profile used for the "no damage" simulation of the Pine Island Glacier shelf. As mentioned in the methods section (3.3), this was created by using the average surface temperature from Comiso (2000) at the surface, assuming 5℃ colder at one third the ice thickness, assuming 0℃ at the base, and fitting a polynomial through those points. It is expected to be warmer than actual temperatures based on comparison to the limited number of borehole temperature measurements in ice shelves (Humbert, 2010; Wang et al., 2022).

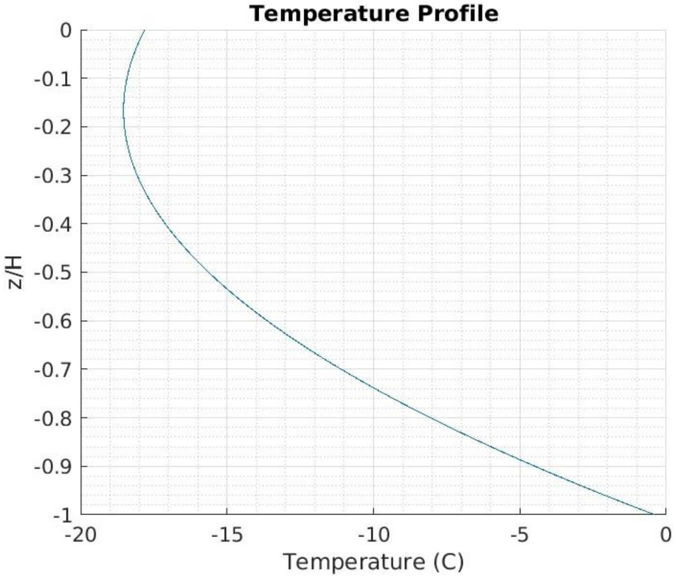

Figure S1: Temperature profile used to calculate the average rigidity for the Pine Island Glacier ice Shelf.

S3: Crevasse Penetration maps for the Pine Island Glacier Shelf

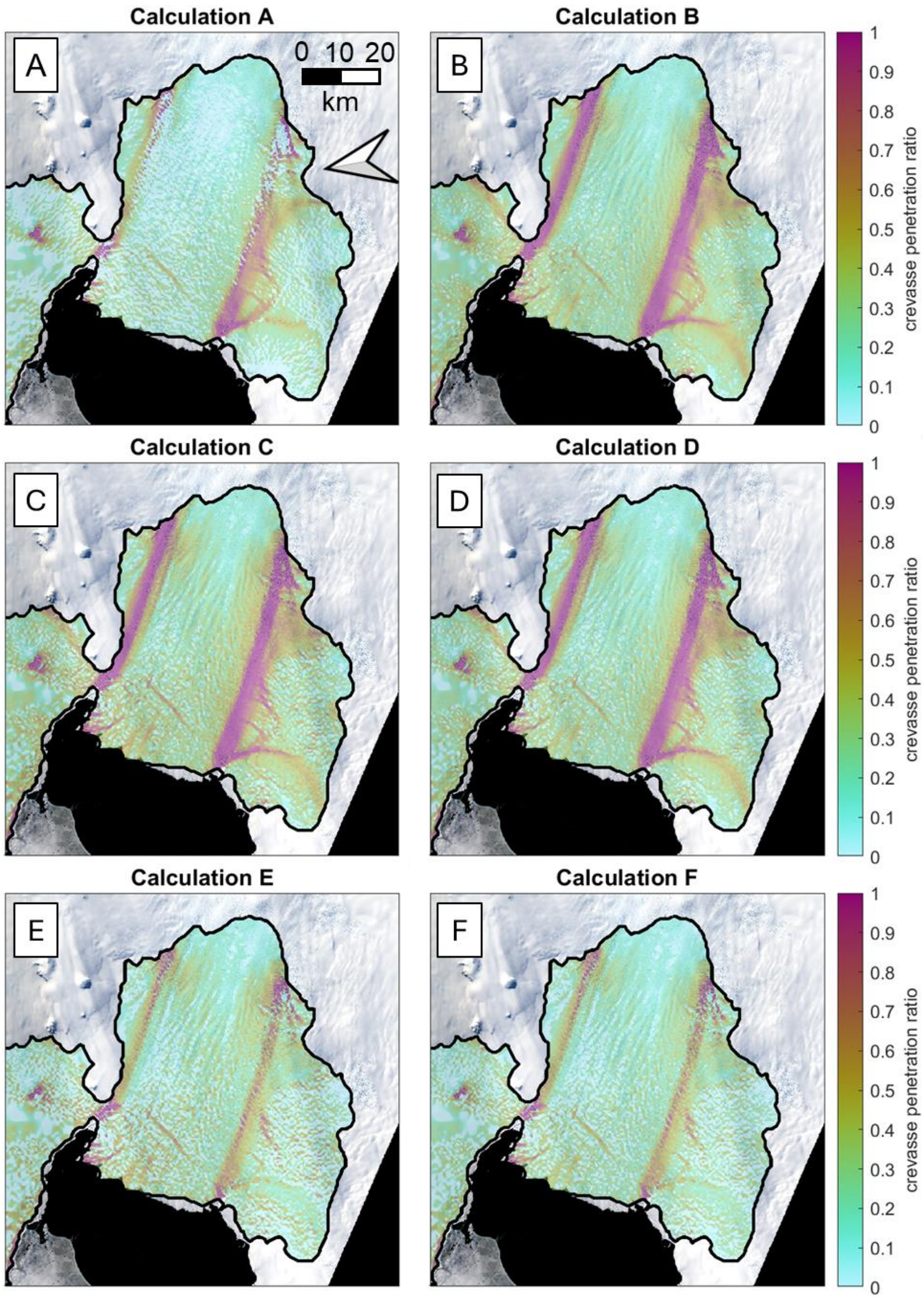

Figure S2: Crevasse penetration at the Pine Island Glacier ice shelf with (A) calculation A, (B) calculation B, (C) calculation C, (D) calculation D, (E) calculation E, and (F) calculation F resistive stress versions overlaid on satellite imagery from November 2014 (Landsat-8 image courtesy of the U.S. Geological Survey). Ice flow direction is approximately from image top to bottom.

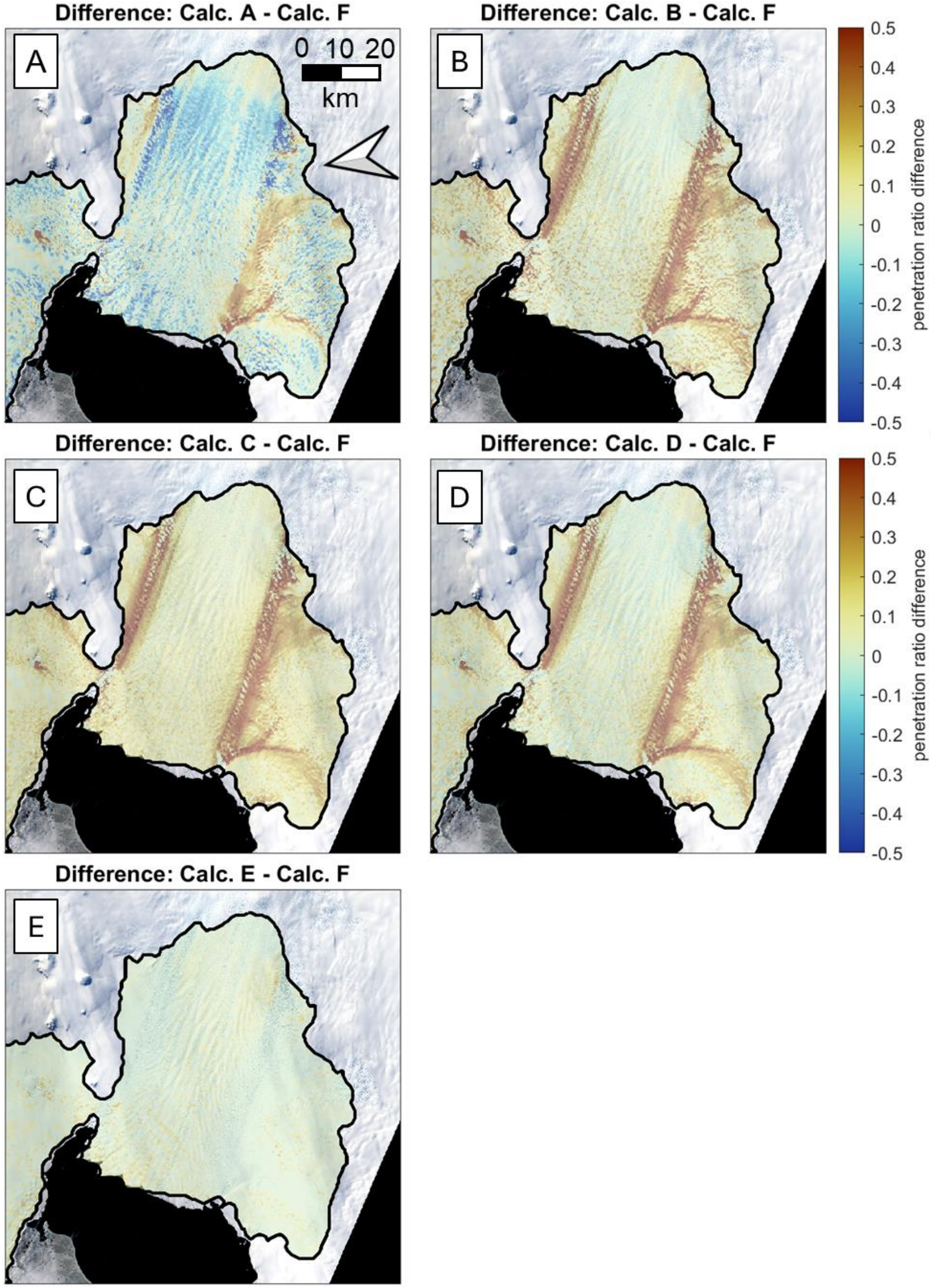

Figure S3: Difference from calculation F crevasse penetration for (A) calculation A, (B) calculation B, (C) calculation C, (D) calculation D, and (E) calculation E crevasse penetration at the Pine Island Glacier ice shelf.

S4: Modelled Velocity Maps for the Larsen B Remnant and Pine Island Glacier ice shelves

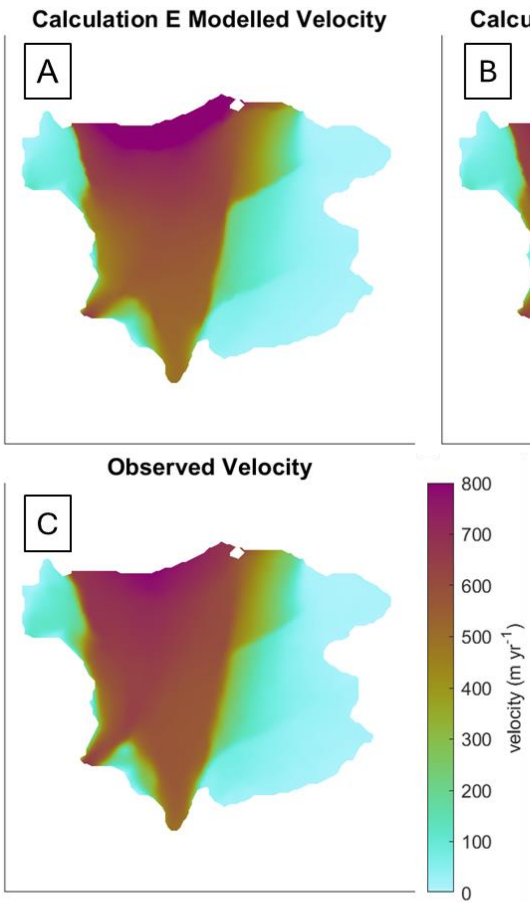

Figure S4: Plots of (A) modelled velocity with calculation E, (B) modelled velocity with calculation F, and (C) observed velocity for the Larsen B remnant ice shelf. The velocity product used for crevasse penetration calculation and shown in (C) is the MEaSUREs 2014-2017 averaged product (Gardner et al., 2018, 2019).

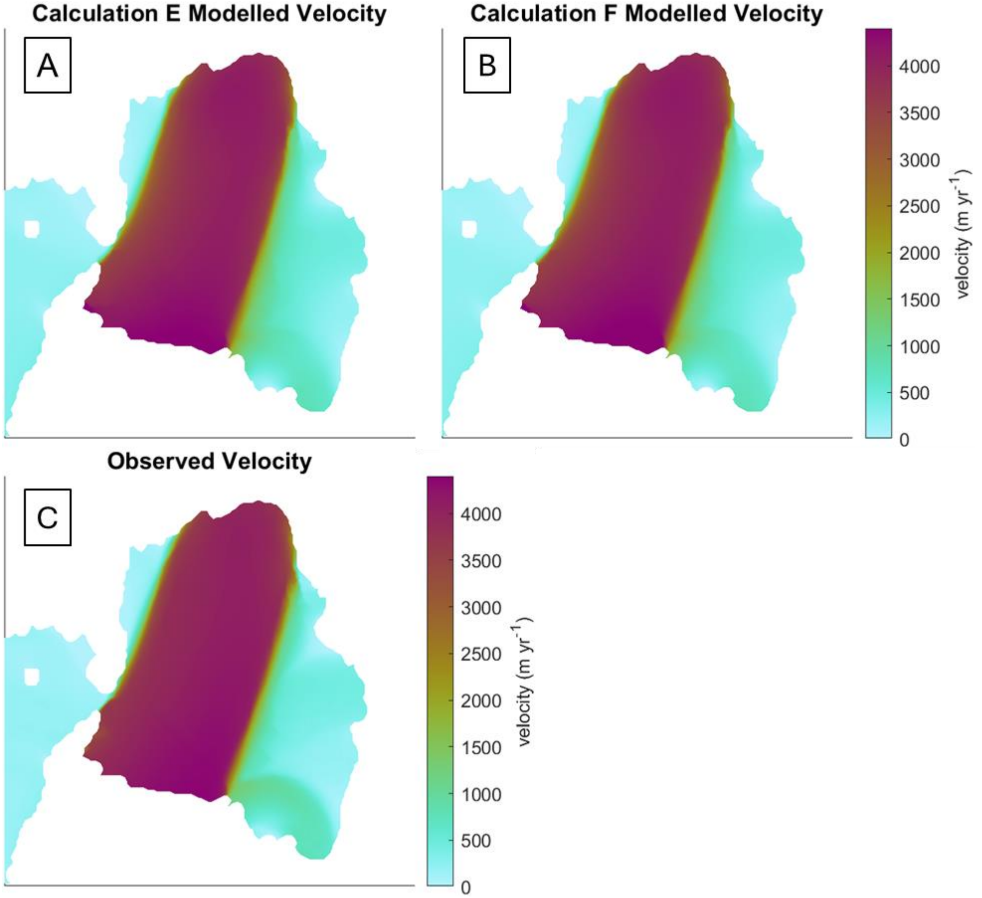

Figure S5: Plots of (A) modelled velocity with calculation E, (B) modelled velocity with calculation F, and (C) observed velocity for the Pine Island Glacier ice shelf. The velocity product used for crevasse penetration calculation and shown in (C) is the ITS_LIVE 2015 annual map (Rignot et al., 2022).

References

Comiso, J. C.: Variability and Trends in Antarctic Surface Temperatures from In Situ and Satellite Infrared Measurements, Journal of Climate, 13, 1674–1696, https://doi.org/10.1175/1520-0442(2000)013<1674:VATIAS>2.0.CO;2, 2000.

Gardner, A. S., Moholdt, G., Scambos, T., Fahnstock, M., Ligtenberg, S., van den Broeke, M., and Nilsson, J.: Increased West Antarctic and unchanged East Antarctic ice discharge over the last 7 years, The Cryosphere, 12, 521–547, https://doi.org/10.5194/tc-12-521-2018, 2018.

Gardner, A. S., Fahnestock, M. A., and Scambos, T. A.: ITS_LIVE Regional Glacier and Ice Sheet Surface Velocities (Version 1), Data archived at National Snow and Ice Data Center [dataset], https://doi:10.5067/6II6VW8LLWJ7, 2019.

Humbert, A.: The temperature regime of Fimbulisen, Antarctica, Annals of Glaciology, 51, 56–64, https://doi.org/10.3189/172756410791392673, 2010.

Lai, C.-Y., Kingslake, J., Wearing, M. G., Chen, P.-H. C., Gentine, P., Li, H., Spergel, J. J., and van Wessem, J. M.: Vulnerability of Antarctica’s ice shelves to meltwater-driven fracture, Nature, 584, 574-+, https://doi.org/10.1038/s41586-020-2627-8, 2020.

Rignot, E., Scheuchkl, B., Mouginot, J., and Jeong, S.: MEaSUREs Multi-year Reference Velocity Maps of the Antarctic Ice Sheet, Version 1, https://doi.org/10.5067/FB851ZIZYX5O, 2022.

Wang, Y., Zhao, C., Gladstone, R., Galton-Fenzi, B., and Warner, R.: Thermal structure of the Amery Ice Shelf from borehole observations and simulations, The Cryosphere, 16, 1221–1245, https://doi.org/10.5194/tc-16-1221-2022, 2022.